Processing–Morphology–Property Relationships in Epoxy Resins

JOVAN MIJOVIĆ,* *Department of Chemical Engineering, Polytechnic Institute of New York, Brooklyn, New York 11201* and JOHN G. WILLIAMS and TOM DONNELLAN, *Naval Air Development Center, Warminster, Pennsylvania 18974*

Synopsis

An investigation was conducted into processing–morphology–property relationships of a series of epoxy resin formulations. Diglycidyl ether of bisphenol A (DGEBA) epoxy resin was cured with diethylene triamine (DETA) and 2,5-dimethyl 2,5-hexane diamine (DMHDA). The two systems were compared by electron microscopic investigation and thermomechanical and fracture property measurements. Transmission electron microscopy has revealed a difference in the morphology of fracture surfaces. On the other hand, thermomechanical and fracture properties of DETA- and DMHDA-cured formulations were found to be very similar. Three different processing (curing) conditions were used for DMHDA-cured formulations, without an apparent effect on their properties. The previously reported improvement in impact energy of DMHDA-cured formulations is unfounded.

INTRODUCTION

The inherent brittleness of epoxy resins restricts their use as adhesives and/or matrices in composites. In recent years, however, considerable research effort has been expanded in the direction of toughening of epoxy resins. An update on the state-of-the-art of this subject has been presented at the recently held symposium on toughened thermosets.[1] The most common toughening route, i.e., the addition of rubbery phase, leads to an increase in impact strength and, unfortunately, a decrease in T_g and modulus.

An alternative way of increasing the impact energy of an epoxy formulation has been recently reported.[2] The sterically hindered aliphatic amine [2,5-dimethyl 2,5-hexane diamine (DMHDA)] was reported to increase both the impact strength and the glass transition of the cured resin. However, an explanation of these findings on the morphological level has not been advanced. It was also suggested in that study that DMHDA reacts with epoxy by first forming a linear polymer, which undergoes crosslinking only after 50% of epoxide groups have reacted. In such instance, it would appear possible to control the resin morphology (and hence physical/mechanical properties) via changes in the curing agent concentration and cure schedule.

The objectives of this study are to confirm the improved impact strength of DMHDA cured systems and to provide an explanation in terms of changes on the morphological level. The expected significance of this research would be in learning how to tailor-make epoxy resins with desired properties (increased toughness and T_g) from the knowledge of their morphology.

* To whom correspondence should be addressed

Journal of Applied Polymer Science, Vol. 30, 2351–2366 (1985)
 CCC 0021-8995/85/062351-16$04.00

EXPERIMENTAL

Materials

Epon 825, Shell's liquid diglycidyl ether of bisphenol A (DGEBA) epoxy resin, was used in this study. This resin is a purified form of commercially available Epon 826. Diethylene triamine (DETA) and 2,5-dimethyl 2,5-hexane diamine (DMHDA) were used as curing agents. The former was obtained from the Aldrich Chemical Co. and the latter was supplied by the Naval Air Development Center. Chemical structures of the epoxy resin and curing agents are shown in Table I. Eight different epoxy resin formulations were investigated. The code and composition of different formulations are outlined in Table II. All formulations were thoroughly mixed at 20°C and then degassed in vacuum for 5 min. The subsequent curing was conducted in accordance with one of the cure schedules described in Table III.

Techniques

Fracture Property Measurements

Linear elastic fracture mechanics (LEFM) analysis was applied to calculate the fracture energy of samples prepared in the form of adhesive joints. Height-tapered double cantilever beam (HTDCB) specimens were used for fracture energy measurements. By tapering the specimen height, the strain energy release rate in mode I (G_I) becomes independent of the crack length. The preparation of surfaces of HTDCB specimens is described elsewhere.[3] Upon priming, the bonding surfaces were ready for the application of adhesive. Resin and curing agent were then mixed, applied onto beams,[4] and further cure was conducted as outlined in Tables II and III. The HTDCB samples were fractured in an Instron tensile tester at room temperature and at a crosshead speed of 0.05 in./min. The calculation of the critical strain energy release rate was performed as described elsewhere.[4]

Impact Strength Measurements

Izod impact tests were conducted on specimens cut from sheets of cured resin, uniform in thickness and free from defects. Specimens were cut to size (2.5 × 0.5 × 0.125 in.) using a Felker Bay State/Dresser 41-AR diamond blade bench saw. A sharp crack was introduced in the specimen, resulting in higher stress concentration at the crack tip, which provides a more realistic lower limiting value of the impact strength. Tests were conducted on a Wiedemann Baldwin impact tester (Wiedeman Machine Co.) following the procedure outlined in ASTMD-25681 Method A.

Electron Microscopy

Approximately 1 × 1 × 0.3 (cm) samples for scanning electron microscopy (SEM) were mounted with a conductive cement onto scanning electron microscope specimen stubs. Samples were then rotated and shadowed with gold at pressure of less than 10^{-5} torr. CVC CVE-14 evaporator was used

TABLE I
Chemical Structure of Epoxy Resin and Curing Agents

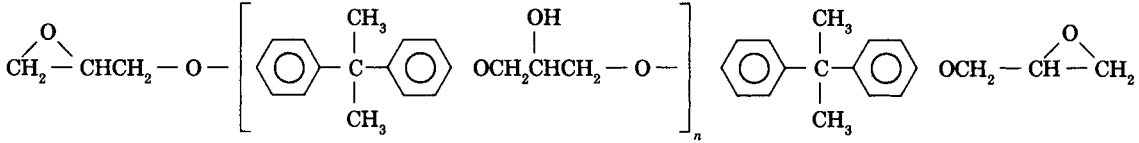

Typical diglycidyl ether of bisphenol A (DGEBA) Resin

Diethylene triamine (DETA) Curing agent

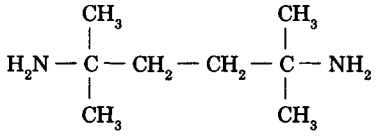

2,5-Dimethyl-2,5-hexane diamine (DMHDA) curing agent

TABLE II
Various Epoxy Resin Formulations Studied

Formulation code	Composition	Cure schedule[a]
1	Epon 825 + 16 phr[b] DMHDA	Intermediate
2	Epon 825 + 21.8 phr DMHDA	Slow
3	Epon 825 + 21.8 phr DMHDA	Intermediate
4	Epon 825 + 21.8 phr DMHDA	High
5	Epon 825 + 25 phr DMHDA	Intermediate
6	Epon 825 + 75/25 DMHDA/DETA	Intermediate
7	Epon 825 + 12 phr DETA	Intermediate
8	Epon 825 + 21.8 phr DMHDA	Intermediate with post-cure

[a] See Table III.
[b] Parts per hundred parts of resin, by weight.

for carbon–platinum (C–Pt) shadowing of fracture surfaces for transmission electron microscopy (TEM). A more detailed schematic representation of the actual shadowing arrangement is given in Figure 1.[5] Successful replicas were made of areas near the tapped-in precrack to the end of the specimen, from one end to the other along the specimen width and from both sides of the crack front. Electron microscopes used throughout this study include JEOL100B and AMR-1200 scanning electron microscopes and JEOL100B, JEOL100C, and Philips EM200 transmission electron microscopes.

Differential Scanning Calorimetry (DSC)

Samples for the DSC analysis were taken from the fracture surfaces on HTDCB specimens. Tests were run in DuPont 910 DSC Module connected to 1090 Thermal Analyzer. All tests were run in nitrogen atmosphere at a heating rate of 10°C/min.

TABLE III
Various Cure Schedules Employed in This Study

1. Slow	Components mixed at RT, subject to vacuum for 5 min, then poured into casting dam: 24 h at 20°C 12 h at 60°C 12 h at 90°C 3 h at 130°C
2. Intermediate	Components mixed at RT, subject to vacuum for 5 min, then poured into casting dam: 16 h at 20°C 1 h at 60°C 3 h at 130°C
3. High	Components mixed at RT, subject to vacuum for 5 min, then poured into casting dam maintained at 60°C: 4 h at 60°C 2 h at 90°C 3 h at 130°C
4. Intermediate with post-cure	Same as intermediate plus additonal: 2 h at 150°C

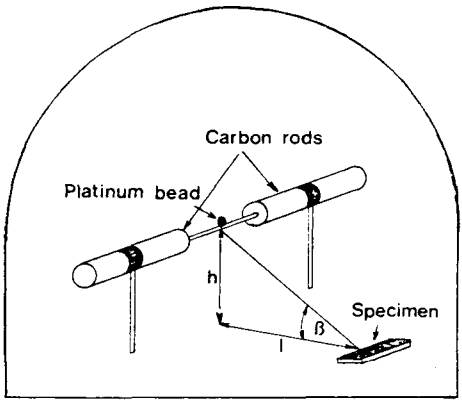

Fig. 1. Carbon–platinum (C–Pt) shadowing setup inside the bell jar. Approximate dimensions: $h = 4$–5 cm, $l = 8$–10 cm.

Dynamic Mechanical Analysis (DMA)

Specimens for dynamic mechanical measurements were cast in silicone rubber molds. A Silastic E RTV rubber (Dow Corning) cured with 10 parts per hundred parts of resin, by weight (phr) of Silastic E curing agent was used for the preparation of molds. Dynamic mechanical measurements were performed in DuPont DMA 981 Module connected to 1090 Thermal Analyzer. All tests were run at the oscillation amplitude of 0.2 mm peak-to-peak and heating rate of 5°C/min.

RESULTS AND DISCUSSION

We begin our discussion by presenting Table IV, which summarizes the data on fracture mechanics and thermomechanical analysis for the eight systems under investigation.

TABLE IV
Summary of Values of Critical Strain Energy Release Rate for Crack Initiation and Glass Transition for Various Formulations

				T_g (°C), days after cure			
Formulation	G_{Ici}[a] (J/m²)	G_{Ica} (J/m²)	Fracture surface	6 days	15/19[b] days	Rerun 15/19[b] days	Additional post-cure 19th day 2 h at 150°C
1	129	42	CoB[c]	68	63	—	93
2	97	34	CoB	117	100	—	134
3	101	26	CoB	111	120	137	145
	137	145					
4	99	34	CoB	118	127	140	139
5	172	59	CoB	114	107	108[b]	128
6	130	24	CoB	121	120[b]	128	—
7	105	40	CoB	105	—	—	118
8	122	40	CoB	—	—	—	—

[a] G_{Ic} are average values of at least six tests.
[b] T_g measured after 19 days.
[c] CoB = center of bond failure.

Fracture Studies

Immediately upon the extension of the tapped-in precrack, samples were unloaded, then reloaded till the critical load for crack initiation (Pc_i), and the load crack arrest (Pc_a) values were obtained. This procedure was repeated to obtain as many data points as possible. Only samples that gave at least three data points within the tapered region were taken into account for the calculations. The first crack obtained by tensile loading was assumed to be the extension of the precrack and was not included in the calculations. It was also assumed that the first crack was sharp enough to be a natural crack.

Almost all fracture specimens exhibited an apparent cohesive [center of bond (CoB)] failure. Ocassionally, a crack was found to propagate (over a short distance) along the resin–metal interface, but such points were not considered for the calculations of strain energy release rate. The crack propagation path was observed to migrate between the aluminum adherends, although the fracture remained invariably within the adhesive. Each initiation occurred in a plane different from that in which the crack had arrested. Similar experimental results have also been reported by other researchers.[4,6] An analytical study of the effect of crack elevation in the height-tapered double cantilever beam (HTDCB) adhesive test configuration showed that the crack growth angle increases with respect to its original plane, as the crack approaches the adhesive–adherend interface.[7]

The first set of experiments focused on the standard DGEBA/DETA (formulation 7) and DGEBA/DMHDA (formulations 3 and 8) systems. The three formulations were prepared by using (a) the stoichiometric ratio of curing agent and (b) the identical curing schedule. The only difference was that formulation 8 was also exposed to an additional post-cure of 150°C for 2 h.

Little difference was noted between the fracture energies of the three systems, as clearly seen in Table V. The DGEBA/DETA system cured in this manner is known to be fully cured.[8] It was suggested that the DGEBA/DMHDA system must be cured at 150°C/2 h in order to obtain a "fully cured" network. However, we did not observe a meaningful difference in G_{Ic}'s of samples with and without post-cure (formulations 3 and 8). Hence the fracture energy measurements failed to reveal any difference between the fully cured DGEBA/DETA system and DGEBA/DMHDA systems (with and without post-cure). We next focused our attention upon various DGEBA/DMHDA formulations.

The effects of varying (a) curing agent concentration (Table II) and (b) curing rate schedule (Table III) were examined. In the view of the tendency

TABLE V
Fracture Energy of Standard DGEBA/DMHDA and DGEBA/DETA Formulations

Formulation	Curing agent concentration (phr)	Cure schedule	G_{Ici} (J/m^2)
3	21.8 (DMHDA)	Intermediate	101
7	12.0 (DETA)	Intermediate	105
8	21.8 (DMHDA)	Intermediate with post-cure	122

of DGEBA/DMHDA formulations to initially form linear polymers, one would expect the variations in curing agent concentration and curing rate to affect the resulting network morphology, and hence properties. Tests were conducted on three different curing agent concentrations and four different cure schedules. The effect of curing agent concentration is seen in Table VI; G_{Ic} passes through a minimum. For the lower curing agent concentration system, the unreacted groups will decrease the average cross-link density and thus increase the fracture energy. The higher curing agent concentration system contains an excess of amine, which could act as a plasticizer. This, in turn, results in a higher value of fracture energy than that obtained with the exact stoichiometric ratio of curing agent. Of course, the unreacted amine groups can react with groups other than epoxy, which are present in the formulation. The effect of curing schedule is also seen in Table VI. One can conclude, considering the variation in experimental results, that G_{Ic} does not change as a function of cure schedule. This observation suggests that only insignificant changes (with respect to fracture energy) occur in the epoxy resin morphology as a function of cure schedule. Finally, it is worth noting that formulation 6 (cured with the 75/25 DMHDA/DETA mixture containing the stoichiometric amount of amine) showed slightly higher fracture energy than either formulation 3 or formulation 7.

The results of impact tests conducted on formulations 3 (DGEBA/DMHDA) and 7 (DGEBA/DETA) are shown in Table VII. The impact strengths are quite similar when either curing agent is used. The value of 14.82 J/m for formulation 7 is slightly higher than the previously reported value (11.7 J/m) for the DGEBA/DETA system.[9] On the other hand, the impact strength of formulation 3 is approximately *60% lower* than the 36.6 J/m value reported by Rinde et al.[2]

Thermomechanical Studies

The thermomechanical characteristics of DGEBA/DETA and DGEBA/DMHDA formulations were first compared using dynamic mechanical measurements. Plots of storage modulus (E'), loss modulus (E''), and tan δ as a function of temperature, are shown in Figures 2 and 3 for δ formulations 3 and 7, respectively. The glass transition temperature, as defined by the

TABLE VI
The Effect of Varying Curing Agent Concentration and Cure Schedule on Fracture Energy of DGEBA/DMHDA Formulations

Formulation	Curing agent concentration (phr)	Cure schedule	G_{Ici} (J/m^2)
1	16.0	Intermediate	129
3	21.8	Intermediate	101
5	25.0	Intermediate	172
2	21.8	Slow	97
3	21.8	Intermediate	101
4	21.8	High	99
8	21.8	Intermediate with post-cure	122

TABLE VII
Impact Strength of Standard DGEBA/DMHDA and DGEBA/DETA Formulations

Formulation	Curing agent concentration (phr)	Cure schedule	Impact strength (J/m)[a]
3	21.8	Intermediate	14.06
7	12.0	Intermediate	14.82

[a] Values are averages of at least 10 tests.

location of the α peak in the loss modulus curve, was found to be 148°C for *both* formulations.

We then continued to investigate changes in T_g as a function of curing agent concentration and cure schedule, by differential scanning calorimetry. Values of T_g of various formulations, measured five days after completion of cure, are summarized in Table VIII. A typical DSC thermogram of formulation 4 (rerun) is shown in Figure 4. Interestingly, upon additional post curing at 150°C, the T_g of the DGEBA/DMHDA systems was found to increase. Two different post-cure treatments were used: (1) 2 h at 150°C and (2) an induced post-cure caused by heating in the DSC cell curing the actual test from 30°C to 200°C (at 10°C/min). Changes in T_g caused by these additional post-cure treatments and measured at various times after post-cure, are summarized in Table IX. It is worth noting that the entire 2-h exposure to 150°C does not appear to be crucial for obtaining the ultimate T_g. The latter increases to approximately the same value as a consequence of the heating of the sample to 200°C at 10°C/min, in much less than 2 h. It should also be pointed out that, nevertheless, the post-cure temperature

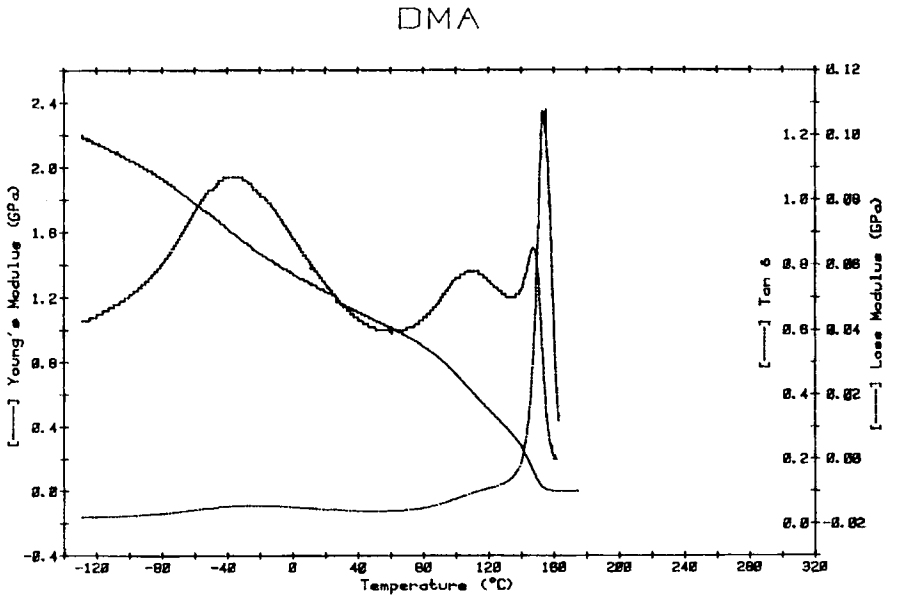

Fig. 2. Dynamic mechanical spectrum of formulation 3 (DGEBA/DMHDA).

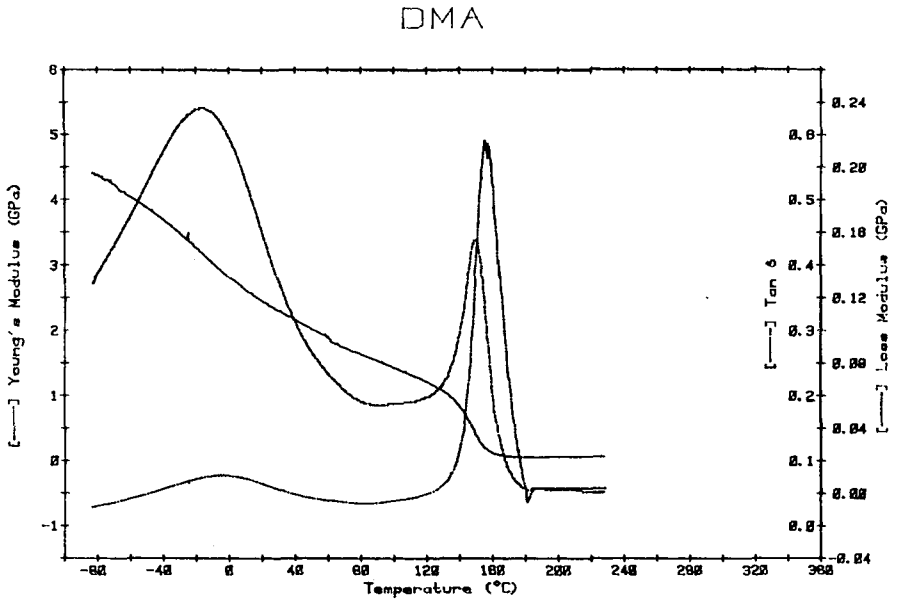

Fig. 3. Dynamic mechanical spectrum of formulation 7 (DGEBA/DETA).

of at least 150°C is needed to obtain the T_g (as measured in DSC) of 142°C. The latter value was reported in the literature[2] as a result of cure at 130°C, a clear difference with our findings.

Electron Microscope Studies

The results of our electron microscopic investigation are discussed next. We reiterate that our primary concern here was the question whether the use of DMHDA instead of DETA will produce noticeable morphological difference. Scanning electron microscopy was used first. We first looked at the fracture surface of formulation 7 (DGEBA/DETA) which has been previously described in the literature.[4,10] The fracture was characterized by distinct zones of crack initiation, propagation, and arrest. Scanning electron micrograph shown in Figure 5 depicts the crack initiation zone. Apparently,

TABLE VIII
The Effect of Varying Curing Agent Concentration and Cure Schedule on T_g

Formulation	Curing agent concentration (phr)	Cure schedule	T_g (°C)
1	16.0	Intermediate	68
3	21.8	Intermediate	111
5	25.0	Intermediate	114
2	21.8	Slow	117
3	21.8	Intermediate	111
4	21.8	High	118
6	75/25	Intermediate	105
7	12.0	Intermediate	121

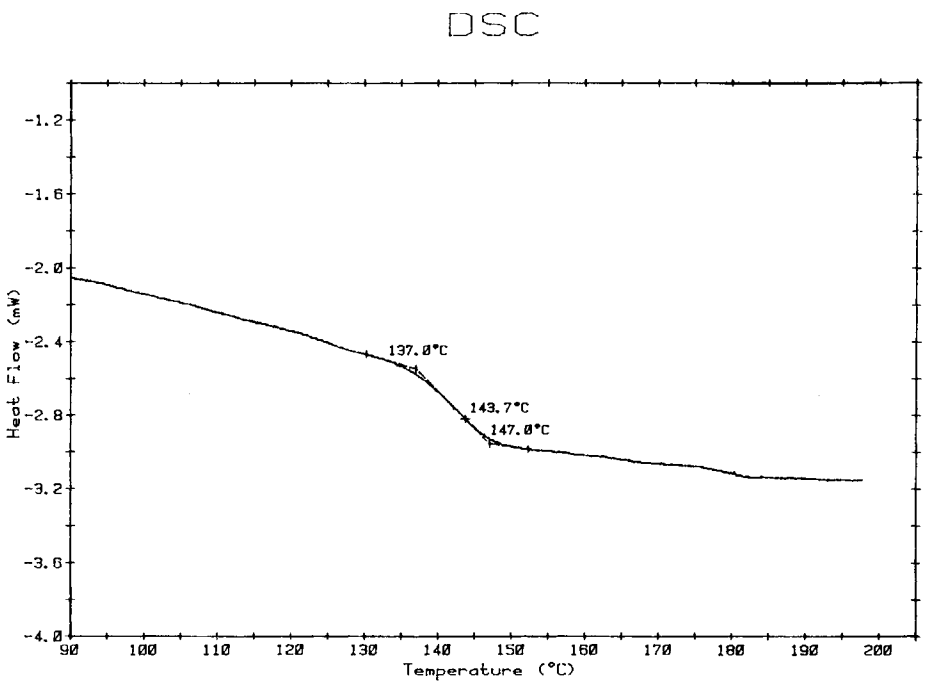

Fig. 4. DSC thermogram of formulation 3 (DGEBA/DMHDA).

the fracture process initiates at many sites along the width of the sample. This probably indicates the presence of "weak" spots in the network such as flaws (microscopic) or areas of locally low crosslink density. Similar morphology was observed in the regions of crack propagation and arrest. The crack initiation zone of formulation 3 was less rough. Some roughness, in the form of crack branching, was observed in the arrest zone but the propagation zone was featureless.

Transmission electron microscopy of formulation 7 has revealed nodular character of the fracture surface as shown in Figure 6. The average nodule size was calculated to be approximately between 15 and 23 nm which is in good agreement with previously published results.[10] Formulation 3 (DGEBA/DMHDA) was studied next, and the difference in morphology was noted. The fracture surface is characterized by a more homogeneous (not nodular) subsurface and a random nodular protrusions (frequently observed on many but not all samples) which range from 22 to 30 nm in diameter, as shown in Figure 7. Upon the subsequent post-curing (formulation 8), there was no evidence of nodular features, as shown in Figure 8. Although the surface possesses a certain degree of roughness, we were not able to detect morphological inhomogeneities. Apparently, the post-cure sequence has an affect on the morphology. One should recall that a simultaneous increase in T_g (Table IX) and a small increase (!) in G_{Ic} were also noted. Intuitively, we did not expect the observed increase in G_{Ic} (even a small one), but one must be careful not to put emphasis on it in the view of variations in results of fracture tests. Naturally, the similarity in thermomechanical and fracture properties of formulations 3 and 7, and the observed difference in their

TABLE IX
Summary of Values of Glass Transitions for Various Formulations

Formulation	Days after cure	T_g (°C)			
		First run	Rerun	Post-cure 18th day 2 h at 150°C, first run	Same post-cure rerun
1	5	68			
	14	63			
	18			93	
2	5	117			
	14	100			
	18				134
3	5	111			
	7		137		
	7[a]	128			
	14	120			
	14		137		
	18			145	
	18				140
4	5	118			
	15	127			
	15		140		
	19			139	
	19				138
5	5	114			
	14	107			
	18		108		
	18				128
6	5	105			
	7			113	
	18			118	
7	5	121			
	18	120			
	18		128		
	18			138	
	26[a]	136			

[a] Sample taken from Izod specimen.

morphologies are not contradictory facts. The difference in the chemical structure of curing agents may give rise to dissimilar morphologies and similar mechanical properties.

Additional information was obtained from the electron microscopy of other formulations. The effect of curing rate on resin morphology was considered first. For instance, interesting observations were made in formulation 2 which was exposed to the lowest initial cure temperature. Parts of the crack initiation zone were similar to those observed in DETA-cured samples (formulation 7). Examples of step formation were detected, preceded by a considerable local plastic deformation, again similar to previously published results in DGEBA/DETA systems.[10] Interestingly, the crack propagation zone is characterized by a random appearance of nuclei, sites where the resin network appears shattered, as shown in Figure 9. Also seen in Figure 9 are long fracture streamlines which originate in the above-men-

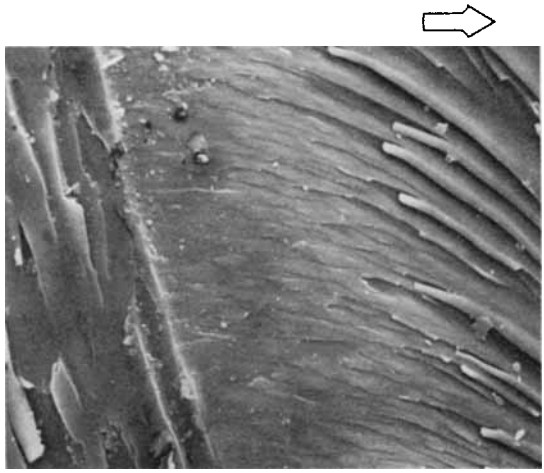

Fig. 5. SEM micrograph of the initation zone on fracture surface of formulation 7. In all micrographs, arrows indicate direction of crack propagation.

tioned nuclei. This formulation was cured initially at a relatively low temperature for a prolonged period of time, and it was previously suggested that such curing conditions would favor the formation of linear polymer. Hence, the structure could be preformed, and in the subsequent curing steps it is possible that the diffusion-controlled reactions and steric hindrance result in the creation of network containing "weak" spots, where the observed fracture nuclei form. High resolution microscopy revealed somewhat rougher surface than in the case of sample cured in intermediate cycle. Formulation 4, which was cured at high initial temperature, shows characteristic fracture streamlines in the initiation zone (Figure 10), but most parts are featureless, i.e., apparently very brittle. The fracture nuclei,

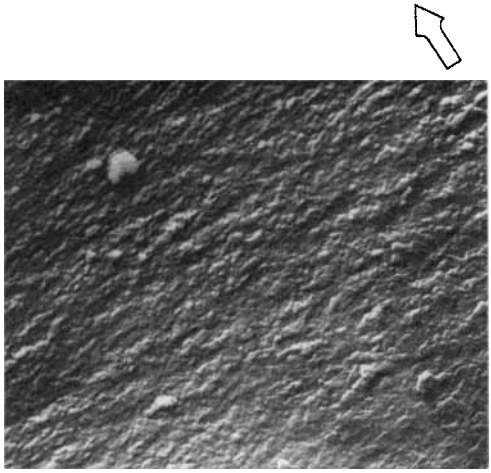

Fig. 6. TEM micrograph of C–Pt replica of fracture surface of formulation 7. Magnification 67,000.

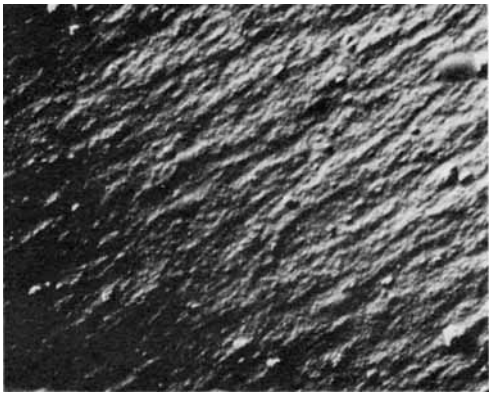

Fig. 7. TEM micrograph of C–Pt replica of fracture surface of formulation 3. Magnification 48,000.

similar to those detected in the crack propagation zone of formulation 2, are here seen only in the initiation and arrest zones. This fracture characteristic is very interesting and quite unique. The crack propagation zone is apparently very brittle and contains only sporadic streamlines with very sharp edges. TEM has revealed grainy but basically featureless fracture surface with no evidence of pronounced inhomogeneities. Actually, the observed fracture surface is very similar to that of formulation 8 (Fig. 8).

The next step in our microscopic investigation was the study of fracture morphology as a function of the curing agent concentration. Formulation 1 is characterized by rougher surface than formulation 3. This is not surprising considering that the deficiency of amine is likely to yield a lower crosslink density network. A clear indication of plastic flow prior to fracture is given in Figure 11. Further confirmation of surface roughness came from TEM. In Figure 12, we have detected surface features of various shape, ranging in size from 45 to 150 nm. The latter entities are rather large aggregates. Formulation 5, cured with the highest concentration of curing agent, was very brittle. Occasional fracture streamlines with sharp edges

Fig. 8. TEM micrograph of C–Pt replica of fracture surface of formulation 8. Magnification 58,400.

Fig. 9. SEM micrograph of the propagation zone on fracture surface of formulation 2.

were seen in the crack initiation zone. The fracture surface observed in TEM micrographs was characterized by an absence of distinct nodules.

Finally, formulation 6 (cured with the 75/25 DMHDA/DGEBA mixture containing the stoichiometric amount of amine) was investigated. Considerable surface roughness was detected, which could be correlated to the observed (although small) increase in G_{Ic} in comparison with formulations 3 and 7 (Table IV). Examples of local plastic flow were found in the crack initiation zone, with numerous fracture streamlines extending well into the crack propagation zone. Surface roughness was also detected in TEM micrographs, but distinct inhomogeneities were not seen.

CONCLUSIONS

We have completed an investigation into processing–morphology–property relationships of various epoxy resin formulations. The emphasis in this

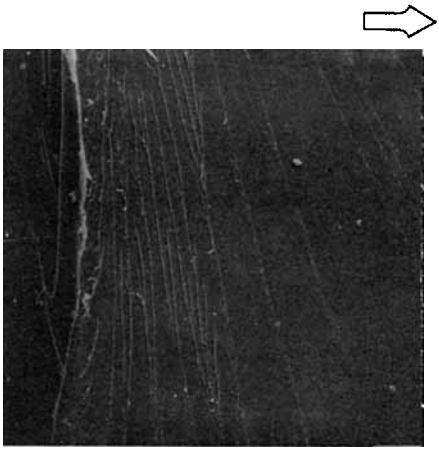

Fig. 10. SEM micrograph of the initiation zone on fracture surface of formulation 4.

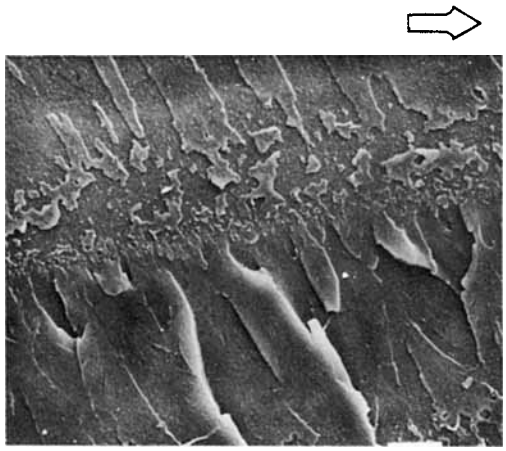

Fig. 11. SEM micrograph of the initiation zone on fracture surface of formulation 1.

study was on the comparison between the characteristics of DGEBA/DETA and DGEBA/DMHDA formulations. The morphology of the two formulations, as seen in transmission electron micrographs, was slightly different. Small, roughly nodular entities were seen in the DETA-cured formulations. There was no evidence of the presence of pronounced regular inhomogeneities on the fracture surfaces of DMHDA-cured formulations. The observed difference in morphology is not surprising considering the difference in the chemical structure of curing agents.

Thermomechanical and fracture properties of the two formulations were found to be very similar, and unaffected by the change in processing (curing) conditions. A large increase in impact energy of the DMHDA-cured formulation, reported elsewhere, has not been confirmed in our study.

This work was supported by the Naval Air Development Center under the Contract N62269-83-M-3261.

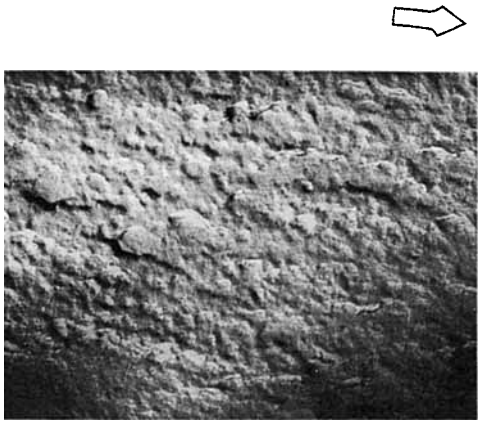

Fig. 12. TEM micrograph of C–Pt replica of fracture surface of formulation 1. Magnification 67,000.

References

1. Symposium on Rubber-Modified Thermoset Resins, in Division of Polymeric Materials Science Engineering Preprints, Vol. 49, 186th National Meeting of Am. Chem. Soc., Washington, D. C., August 1983.
2. J. A. Rinde, I. Chiu, E. T. Mones, and H. A. Newey, *SAMPE Q.*, (Jan.), 22–31 (1980).
3. J. Mijović, *Ind. Eng. Chem. Prod. Res. Dev.*, **21**(2), 290 (1982).
4. J. Mijović, *J. Appl. Polym. Sci.*, **25**, 1179 (1980).
5. J. Mijović and J. A. Koutsky, *J. Appl. Polym. Sci.*, **23**, 1037 (1979).
6. S. Mostovoy, C. R. Bersch, and E. J. Ripling, *J. Adhesion*, **3**, 125 (1971).
7. S. S. Wang, J. F. Mandell, and F. J. McGarry, Research Report R 76-3, MIT, 1976.
8. J. Mijović and L. Tsay, *Polymer*, **22**, 902 (1981).
9. H. Lee and K. Neville, *Handbook of Epoxy Resins*, McGraw-Hill, New York, 1967.
10. J. Mijović and J. A. Koutsky, *Polymer*, **20**(9), 1095 (1979).

Received August 7, 1984
Accepted September 11, 1984